



“Gheorghe Asachi” Technical University of Iasi, Romania



STUDY ON SOLID/LIQUID RATIO AND MICROSTRUCTURE PROPERTIES OF ALKALI-ACTIVATED METAKAOLIN-BASED GEOPOLYMER CONTAINED IN LCD WASTE GLASS

Kang-Wei Lo^{1,2}, Kae-Long Lin^{3*}, Ta-Wui Cheng², Wei-Hao Lee²

¹Graduate Institute of Engineering Technology, National Taipei University of Technology, Taipei City, 106, Taiwan, R.O. C.

²Institute of Mineral Resources Engineering, National Taipei University of Technology, Taipei City, 106, Taiwan, R.O. C.

³Department of Environmental Engineering, National Ilan University, Ilan City, 260, Taiwan

Abstract

There are considerable environmental and health and safety concerns regarding liquid crystal display (LCD) waste glass because of the waste electrical and electronic equipment (e-waste) that is deposited in landfills. In current study, the effect of variation in LCD waste glass on the deconvoluted fractions of silicon centers of metakaolin geopolymers has been comprehensively investigated to discover the underlying mechanisms governing the performance. Solid/liquid ratio affects the kinetics of the exchange of silicate units between species during geopolymerization. Flexural strength is related to the degree of geopolymerization and the number of soluble aluminosilicates in the geopolymer system. The solid/liquid ratio was increased from 0.8 to 1.0, the weight loss of 10% geopolymer in the 230–400 °C decreased from 16.97% to 14.94% at 60-day of curing. Nevertheless, the weight loss from 600–750 °C increased from 0.55% to 0.85%. When the solid/liquid ratio was increased from 0.6 to 1.0, the fractions of Q⁴(3Al) (30.13%–35.07%) and Q⁴(2Al) (30.40%–35.13%) increased, whereas the fractions of Q⁴(4Al) (23.36%–22.57%) and Q⁴(1Al) (10.15%–9.57%) decreased. Geopolymer with 10%–40% LCD waste glass and a solid/liquid ratio of 1.0 can partially replace metakaolin as geopolymer exhibit favourable mechanical characteristics.

Keywords: deconvoluted fractions, geopolymer, liquid crystal display waste glass

Received: April, 2019; Revised final: July, 2019; Accepted: September, 2019; Published in final edited form: January, 2020

1. Introduction

The liquid crystal display (LCD) glass contain complex layers of multiple organic films, semiconductors, electrodes and terminals. As of 2017, LCD waste glass was generated approximately 1.4×10^7 tonnes in use worldwide (Gao et al., 2018; Tadashi, 2016). Fan and Li (2013) indicated that the waste Electrical and Electronic Equipment (e-waste) must be recycled to reduce the amount of e-waste that is deposited in landfills (Chen et al., 2019; Fan and Li, 2013).

Geopolymers are synthetic inorganic materials formed through alkali solution activation of

aluminosilicates. The polymerization produces a three-dimensional (3D) comprising [AlO₄] and [SiO₄] tetrahedrons (Elyamany et al., 2018; Leay et al., 2018). Geopolymerization process starts with aluminosilicate oxide or silicon oxide bonds monomers (oligomers) in solution, which join to form geopolymer with properties similar to those of the Ordinary Portland Cement (OPC) (Bai et al., 2018; Ma et al., 2018; Wang et al., 2016).

Geopolymers have received increasing interest worldwide as an alternative to OPC due to cost increases in energy supply, requirements to reduce CO₂ emission, limited reserve of limestones and limited manufacturing growth of cement (Bergamonti

* Author to whom all correspondence should be addressed: e-mail: kllin@niu.edu.tw; Phone: +886 9317579; Fax: +886 39364277

et al., 2018; Tang et al., 2018; Villaquirán-Caicedo et al., 2018). Geopolymers are considered a promising alternative to OPC in fields such as heat-resistant component manufacturing, hazardous element encapsulation and infrastructure development (Tang, 2018). The mechanical properties of a geopolymer are highly dependent on its composition and curing routes, which in turn are highly dependent on hydroxide concentration, the alkali cation, Si/Al ratio and curing conditions used (Allahverdi et al., 2017; Cheng et al., 2018; Fernández-Pereir et al., 2018; Ghadir and Ranjbar, 2018; Villaquirán-Caicedo et al., 2018). Lin et al. (2012) indicated that the 10% waste glass replacement levels based-metakaolin geopolymer had a strengths of 62 MPa after 60 days of curing (Lin et al., 2012). Lo (2018) indicated that "the geopolymers with 0% LCD waste glass and an $\text{SiO}_2/\text{Na}_2\text{O}$ (S/N) ratio of 2.0 is shown for 60-days of curing had the highest flexural strength (10.4 MPa)" (Lo et al., 2018). El-Naggar and El-Dessouky (2017) reported that the grinding the MK particle size to 38 μm , $\text{SiO}_2/\text{Na}_2\text{O}$ of 1.55, and early age curing at 40 °C. Mechanical properties were 80.75-97.41 MPa (El-Naggar and El-Dessouky, 2017). Bai et al. (2019) indicated that waste glass-based cellular geopolymers with total porosity about ~55 vol%, thermal conductivity of ~0.21 W/mK, and mechanical strength of ~7.3 MPa were successfully produced by a direct foaming technique using hydrogen peroxide in combination with Triton X-100 (Bai et al., 2019). Novais et al. (2016) fluorescent lamps as raw material in geopolymers. Sampled containing 37.5 wt.% waste glass had a compressive strength of 14 MPa (after 28 days of curing), showing the possibility of their use in non-structural application (Novais et al., 2016). Dembovska et al.(2017) reported that the value of different industrial by-products and residues in the production of lightweight alkali activated materials. The results showed that highly porous lightweight building materials could be obtained, with densities ranging from 380 to 470 kg/m^3 , heat conductivities ranging between 0.14 and 0.15 W/mK, and compressive strengths ranging between 1.1 and 2.0 MPa (Dembovska et al., 2017). Wan et al. (2017) reported that metakaolin-based geopolymers were synthesized at Si/Al ratios of 1:1, 1.5:1, 2:1, 3:1, 4:1, and 5:1 by using silica fume as silica corrector to alter Si ratios. In the deconvoluted fractions, $\text{Q}^4(4\text{Al})$ is the main compound in geopolymer of Si/Al ratio 1:1, in which a trace amount of $\text{Q}^4(3\text{Al})$ and $\text{Q}^4(2\text{Al})$ compounds are present. Interestingly, $\text{Q}^2(1\text{Al})$ is found due to the high concentration of aluminate monomers. As increasing the Si/Al ratios from 1.5:1 to 2:1 and 4:1, the fractions of $\text{Q}^4(4\text{Al}+3\text{Al})$ decrease, while the fractions of $\text{Q}^4(1\text{Al}+0\text{Al})$ increase, but the fraction of $\text{Q}^4(2\text{Al})$ shows the maximum at Si/Al ratio of 2:1 (Wan et al., 2017).

The novelty of current work lies firstly in investigating the effect of difference in LCD waste glass and $\text{SiO}_2/\text{Na}_2\text{O}$ ratio on the deconvoluted fractions of silicon centers of metakaolin geopolymers in a systematic and comprehensive way, and secondly

in discovering the underlying mechanisms governing the performance. Geopolymerization reaction was characterized through TG/DTA analysis, and NMR by adopting Gaussian peak deconvolution to quantify Q^n (4Al-0Al) species analysis.

2. Experimental

2.1. Material and methods

The starting materials were metakaolin and LCD waste glass. Metakaolin is obtained from kaolin calcination at 650 °C for three hours. LCD waste glass from Taiwan panel factory. The main chemical composition of LCD waste glass is 52.8% SiO_2 , 13.5% Al_2O_3 and 6.14% CaO ; metakaolin were 49.2% SiO_2 , 48.3% Al_2O_3 . Metakaolin and LCD waste glass were pulverized to a fineness value (on Blaine) of approximately 316 $\text{m}^2/\text{kg}^{-1}$ and 300 m^2/kg , respectively. LCD waste glass is ground to a fineness of 300 m^2/kg approximately. Fig. 1 shows the crystallization of the LCD waste glass was amorphous, and the metakaolin crystals were composed of SiO_2 .

An alkaline solution that contained waterglass (Na_2SiO_3 ; S/N =3.4) (First Chemical Materials Co., Ltd.) and 10M NaOH, with $\text{SiO}_2/\text{Na}_2\text{O}$ ratio was 1.74 and solid-to-liquid ratio was 0.4-1.0. LCD waste glass (0%, 10%, 20%, 30% and 40%), were added into the alkali activator (Hao et al., 2015).

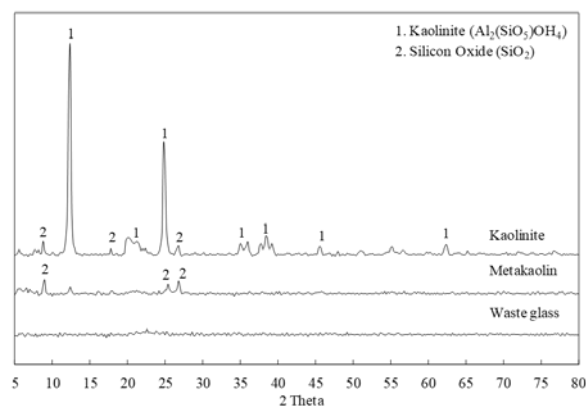


Fig. 1. XRD patterns of raw materials

2.2. Methodology

Solution was prepared using 97% sodium hydroxide pellets (Fisher Scientific) to the 10 M NaOH solution. Geopolymers samples were synthesized by mixing solid powder and activating solution, the paste was poured into cuboid moulds (40^(L) × 30^(W) × 10^(H) mm). After 24 hours, all the geopolymers were removed from the moulds and cured at 30°C The flexural strength tests were performed after 1, 3, 7, 14, 28 and 60 days using a model of Hung Ta HT-2402 testing machine with three-point bending test method, according to ASTM C348. The average strength of the three specimens is

presented. The coefficient of variation of these results was less than 10%. The heat revolution in the geopolymerization reactions, such as dissolution, polymerization and condensation, were characterized by a Calmetrix I-CAL 2000 HPC, with the external temperature maintained at $30 \pm 0.001^\circ\text{C}$. The DTA/TG studies were conducted, which heating range was from 50°C to 1000°C by STA6000 thermal analyzer. ^{27}Al MAS NMR spectra of geopolymers and LCD waste glass -geopolymers were determined with NMR spectroscopy (Bruker MAS/NMR-200) at 39.72 MHz. The lack of spectral resolution for silicon in geopolymers has been overcome by adopting Gaussian peak deconvolution to separate and quantify Q^n ($4\text{Al} - 0\text{Al}$) species ($0 \leq n \leq 4$) as previously reported (Lee and Stebbins, 1999).

The coordination of Q^n ($4\text{Al} - 0\text{Al}$) in metakaolin was obtained by applying Seasolve PeakFit™ software and Gaussian peak deconvolution as reported elsewhere (Wan et al., 2017). NMR studies have shown that all silicon and aluminum sites are in tetrahedral coordination in geopolymers, thus $n = 4$ (Rahier et al., 1996).

3. Results and discussion

3.1. Effects of solid/liquid (S/L) ratios on strength development

In Fig. 2(a) it is reported, the flexural strength development in LCD waste glass geopolymers with an S/L ratio of 0.4. When geopolymer with 0%- 40% LCD waste glass, strength were 1.4, 1.1, 1.0, 0.8, and 0.5 MPa at 1 day of curing, respectively. This shows that strength decreases as the LCD waste glass replacement levels increases. However, Fig. 2(a) clearly showing that the strength for the mix with 0% LCD had flexural strength of about (1.4 to 2.3) MPa during the curing period of 1-7 days. Lin et al. (2012) demonstrated the flexural strength is related to the degree of geopolymerization and the number of soluble aluminosilicates in the geopolymer system. The geopolymers with LCD waste glass replacement levels of 0, 10, 20, 30 and 40% had a strength of 3.5, 2.3, 2.1, 1.9, and 1.2 MPa at 60-day of curing, respectively. Lin et al. (2012) reported that geopolymer that contained TFT-LCD waste glass released fewer silicon and aluminum ions than that which did not contain waste glass. These results are in agreement with the previous work obtained by Lo et al. (Lo et al., 2018).

Fig. 2(b) shows the results of the strength of the LCD waste glass geopolymer with an S/L ratio of 0.6. The strength of the geopolymer whose LCD waste glass replacement amount is 10% is 5.4 MPa when cured for 1 day. The flexural strength increased to 8.9 MPa, exceeding 2.3 MPa of the geopolymer containing 10% LCD waste glass, and the S/L ratio at curing for 60 days was 0.4, as shown in Figs. 2(b) and 2(a), respectively. The enhancement of the strength is obtained for all the LCD waste glass replacement percentages, not only for the geopolymers with 10%.

Figs. 2(c) and 2(d) show the results of the strength of LCD waste glass geopolymers with S/L ratios of 0.8 and 1.0, respectively. For geopolymers with 10% LCD waste glass replacement level at 1-day of curing, the S/L ratio increased from 0.8 to 1.0 showed that strength increase from 5.6 to 8.8 MPa. Increasing the S/L ratio results in an increase in the size of oligomers, affecting the kinetics of the exchange of silicate units between species during geopolymerization, this leads to an increase in the content of silicon dioxide in the system, which in turn enhances the synthesis of geopolymers. On the other hand, the silica content in the system was high that may lead to densification of geopolymer which favourable mechanical strength. At S/L ratio of 1.0, the geopolymers with 10% LCD waste glass replacement level had a maximum strength of 14.5 MPa (after 60 days). Because the chemically reactive CaO content in the LCD waste glass, heterogeneous nucleation-crystallization and aluminosilicate geopolymerization may occur simultaneously. The strength of activated geopolymers was significantly improved by replacing 10% -20% of LCD waste glass. Therefore, Fig. 2(d) showed the strength of geopolymers with 20% LCD waste glass higher than 0% LCD waste glass at 60 days.

3.2. Effects of S/L ratio on TG/DTA curves

Tables 1-4 present the TG/DTA weight loss of the LCD waste glass geopolymers in the range $0-1000^\circ\text{C}$. The weight loss analysis was related to carbonate salt, as shown in region I ($100-230^\circ\text{C}$). The weight loss results corresponded to that of dehydration of the material's macropore structure, as shown in region II ($230-400^\circ\text{C}$). The weight loss results were related to amorphous composition (oligomers), as shown in region III ($400-600^\circ\text{C}$) (Lo et al., 2018). The weight loss results were related to dehydroxylation of the geopolymer gel, as shown in region IV ($>600^\circ\text{C}$). At approximately 650°C , the weight loss results were water is eliminated due to condensation of aluminum or silanol groups on the surface of the structure.

Geopolymerization between the two hydroxyl groups connects them together and the product forms part of the aluminosilicate network structure (Lo et al., 2018). The TG/DTA curves and weight loss of LCD waste glass geopolymers with an S/L ratio of 0.4 are shown in Fig. 3 and listed in Table 1. After 28 days of curing, the geopolymer with LCD waste glass replacement level increased from 10% to 40%, and the weight loss in the temperature range of $230-400^\circ\text{C}$ decreased from 15.42% to 15.19%. The replacement rate of LCD waste glass is 10%, 20%, 30% and 40% of geopolymer reached a marked weight loss of 5.46, 5.20, 5.33, and 6.43 wt.% at $400-600^\circ\text{C}$, respectively (Table 1). The results revealed that when the LCD waste glass replacement level was relatively high, an increase in the LCD waste glass content caused unsatisfactory polycondensation, thus causing oligomers to form geopolymer amount decreased.

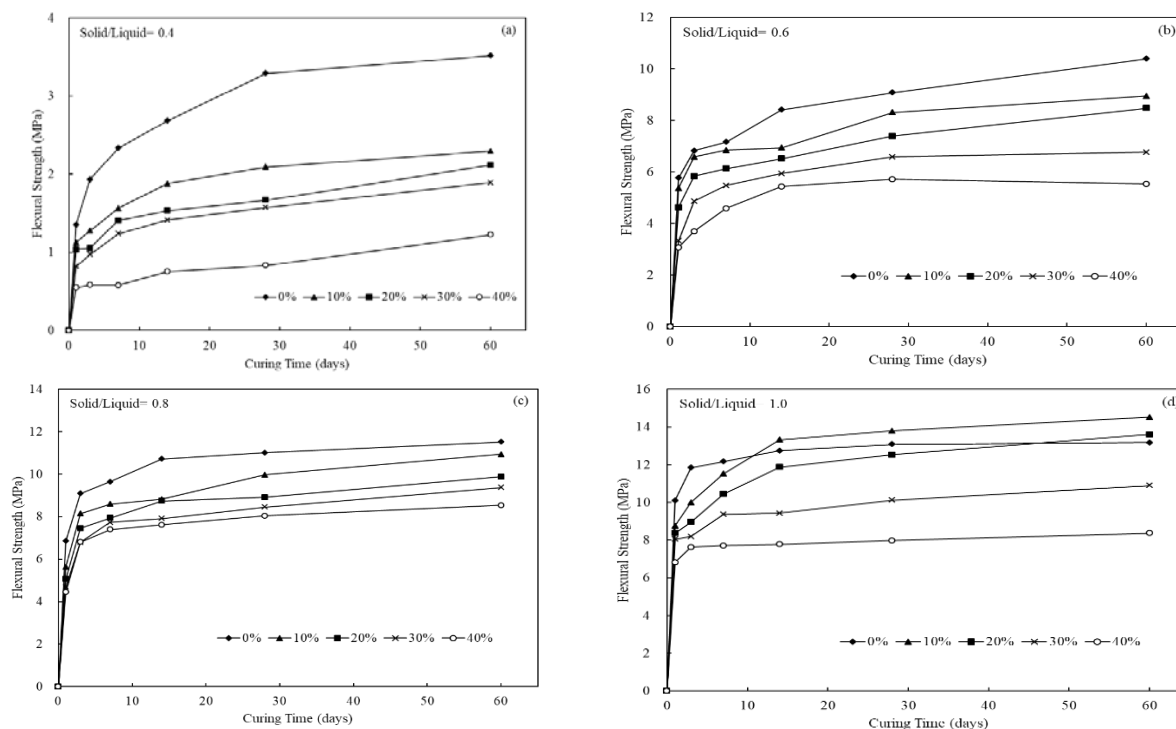


Fig. 2. Effects of S/L ratios on strength development

At 600-750°C temperature range, the weight loss of geopolymers decreased from 2.29% to 1.92%. Similarly, after 60 days of curing, the weight loss increased from 10% to 30% of the waste glass replacement. This performance is attributed to an increase in the amount of waste glass replacement and a decrease in the amount of carbonate formed may be due to the need for more alkali activation of the glass, resulting in a decrease in the amount of carbonate formation. So that, the weight loss of geopolymers with 30% LCD waste glass replacement level increases. Therefore, the weight loss of the geopolymer with an LCD waste glass replacement amount of 30% will increase. As the amount of LCD scrap glass increases, the amount of dissolved Si and Al decreases, led to the geopolymer synthesis reaction were restrained.

Figure 4 and Table 2 show the TG /DTA curve and weight loss of a geopolymer with LCD waste glass when S/L is 0.6. After 60 days of curing, the weight loss at S/L = 0.6 was higher in all cases when the temperature increased from 230-400°C. The results show that in all cases, the weight loss when the S/L ratio is 0.6 is higher than the weight loss when the S/L ratio is 0.4. At 400-600°C temperature range, the weight loss of geopolymers decreased from 4.31% to 3.31% (LCD waste glass replacement level of 10%-40%), as shown in Table 2.

Increasing the S/L ratio promoted the oligomers to form geopolymer the network of Si-O-Al framework structure, thus causing number of oligomers decreased. The TG /DTA analysis of LCD waste glass geopolymers with S/L ratios of 0.8 and 1.0 are shown in Tables 3 and 4, respectively. As shown in Table 2, the TG /DTA curve and weight loss of LCD

waste glass and geopolymer with S/L of 0.6 are shown in Table 2. After 60 days of curing, the total weight loss with S/L ratio = 0.6 is higher when the temperature rises from 230-400°C, S/L = 0.4 is even higher due to enhancement of the polymerization reaction with higher S/L ratio; in the same condition, increasing the S/L ratio from 0.8 to 1.0 the weight loss decreases (Figs. 5 and 6).

As the S/L ratio was increased from 0.8 to 1.0, after a curing time of 60 days, the weight loss of the geopolymers with 10% LCD waste glass replacement level between 230 and 400°C decreased from 16.97% to 14.94 wt.%, as shown in Tables 3-4. However, the weight loss between 600 and 750°C increased from 0.55% to 0.85 wt.% (Table 3 and Table 4). Moreover, the silica content in the system increased with the S/L ratio. The increase in the silica content enhanced the geopolymer synthesis reaction. Consequently, the weight loss in region IV increased. At a S/L ratio of 1.0, the geopolymers with LCD waste glass replacement level of 10%, 20%, 30%, and 40% at 60-day of curing, reached a marked weight loss of 3.66, 3.77, 3.54, and 3.43 wt.% at 400- 600°C, respectively (Table 4). There is not an actual trend in the enhancement of the oligomers content with the increase of the S/L ratio.

3.3. Effects of S/L ratios on ^{27}Al NMR spectra

Figs. 7-10 present the ^{27}Al NMR spectra and deconvolution of LCD waste glass geopolymers with S/L ratios of 0.4, 0.6, 0.8, and 1.0, and the deconvoluted fractions of silicon centers present as $\text{Q}^4(0\text{Al})$, $\text{Q}^4(1\text{Al})$, $\text{Q}^4(2\text{Al})$, $\text{Q}^4(3\text{Al})$, and $\text{Q}^4(4\text{Al})$ (Figs. 11-14).

Table 1. Weight loss analysis of the LCD waste glass geopolymers (Solid/Liquid = 0.4)

Curing Time (days)	Replacement Level (%)	Temperature (°C)			
		100–230	230–400	400–600	600–750
1	0	3.85	16.42	6.11	0.90
1	10	3.84	15.87	5.50	0.56
1	20	3.81	15.08	5.55	0.43
1	30	3.26	14.10	5.11	2.19
1	40	3.18	13.95	5.32	2.62
28	0	4.85	15.71	5.52	2.20
28	10	4.15	15.42	5.46	2.29
28	20	4.59	15.43	5.20	2.28
28	30	4.92	14.97	5.33	2.68
28	40	4.72	15.19	6.43	1.92
60	0	4.40	14.79	4.78	2.14
60	10	3.50	14.62	5.25	2.32
60	20	4.87	14.49	5.45	2.51
60	30	3.27	14.37	5.33	2.73
60	40	5.26	14.42	5.83	2.39

Table 2. Weight loss analysis of the LCD waste glass geopolymers (Solid/Liquid = 0.6)

Curing Time (days)	Replacement Level (%)	Temperature (°C)			
		100–230	230–400	400–600	600–750
1	0	3.24	16.52	4.77	0.91
1	10	3.62	15.95	4.33	0.76
1	20	2.90	15.67	4.50	0.75
1	30	2.58	14.43	4.39	0.70
1	40	2.93	14.02	4.22	1.13
28	0	3.64	18.11	4.75	0.70
28	10	3.77	16.72	4.81	0.96
28	20	3.67	16.48	4.65	0.74
28	30	3.40	16.02	3.94	0.96
28	40	3.16	16.21	4.34	0.82
60	0	3.37	18.82	4.63	0.56
60	10	3.29	17.72	4.31	1.14
60	20	3.28	17.20	3.33	1.04
60	30	3.16	17.16	3.94	1.24
60	40	3.00	16.70	3.31	1.10

Table 3. Weight loss analysis of the LCD waste glass geopolymers (Solid/Liquid = 0.8)

Curing Time (days)	Replacement Level (%)	Temperature (°C)			
		100–230	230–400	400–600	600–750
1	0	3.53	17.29	4.24	0.90
1	10	3.56	16.71	3.99	0.65
1	20	3.14	17.46	3.93	0.55
1	30	2.85	17.56	3.49	0.66
1	40	3.55	15.97	3.65	0.65
28	0	3.43	15.87	4.15	0.63
28	10	4.03	15.87	3.90	0.76
28	20	3.62	16.99	3.59	0.55
28	30	3.63	16.18	2.58	0.55
28	40	3.40	16.81	4.00	0.76
60	0	3.17	15.15	4.26	0.68
60	10	3.20	16.97	2.92	0.55
60	20	2.94	16.78	2.61	0.49
60	30	3.18	16.99	2.58	0.60
60	40	3.20	18.53	2.44	0.71

Table 4. Weight loss analysis of the LCD waste glass geopolymers (Solid/Liquid = 1.0)

Curing Time (days)	Replacement Level (%)	Temperature (°C)			
		100–230	230–400	400–600	600–750
1	0	2.69	13.67	2.94	1.12
1	10	2.62	13.42	3.41	0.61
1	20	2.71	13.66	4.02	0.65
1	30	2.76	13.71	3.81	0.74
1	40	2.79	16.33	3.95	0.76
28	0	2.67	14.92	3.63	1.01
28	10	2.81	14.62	4.07	1.09
28	20	2.90	14.42	3.71	0.83
28	30	2.98	14.24	3.54	0.60
28	40	3.25	14.25	3.93	0.63
60	0	2.78	15.82	3.99	0.88
60	10	2.83	14.94	3.66	0.85
60	20	2.95	14.71	3.77	0.63
60	30	3.05	14.55	3.54	0.62
60	40	3.23	14.92	3.43	0.66

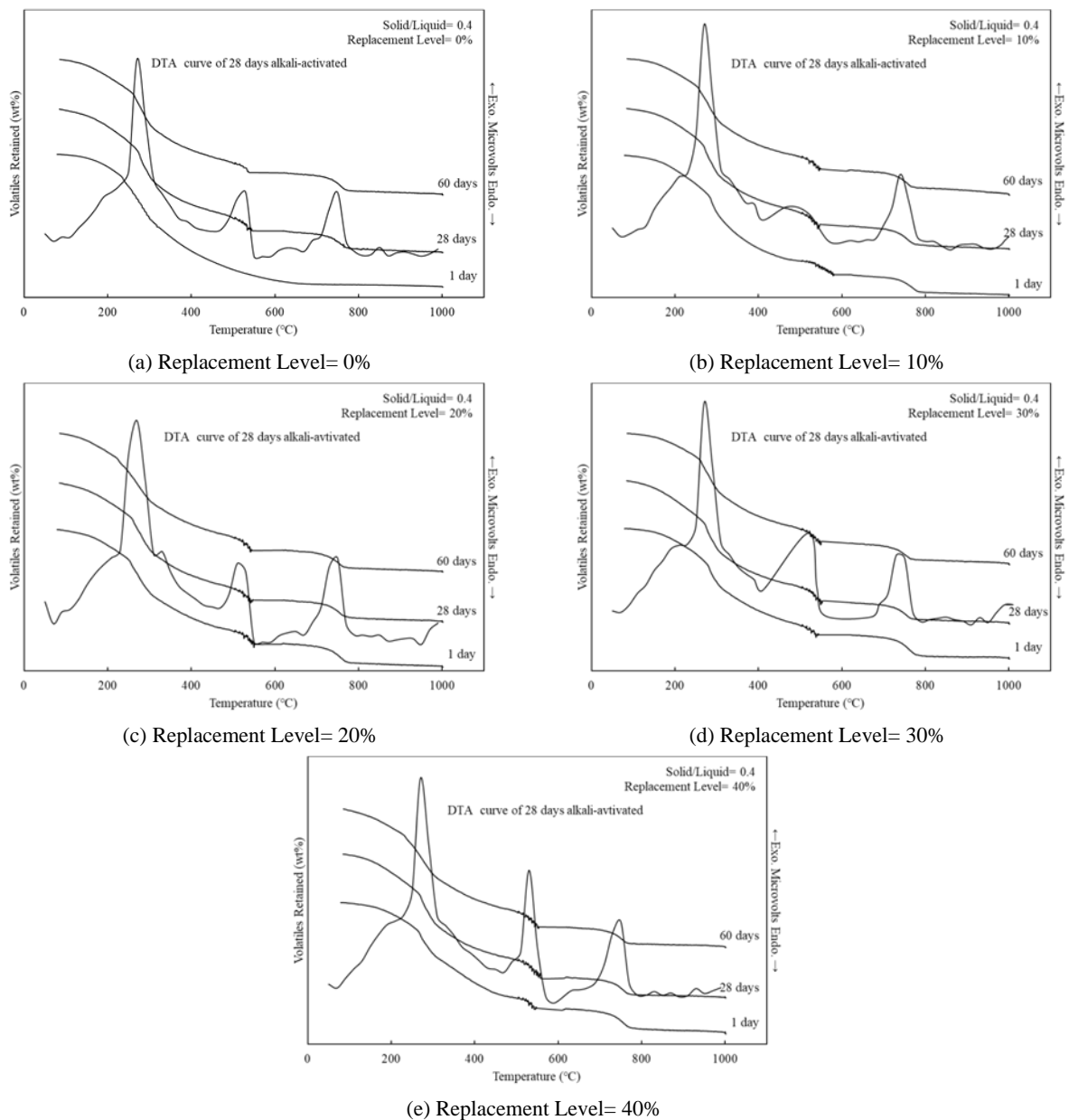
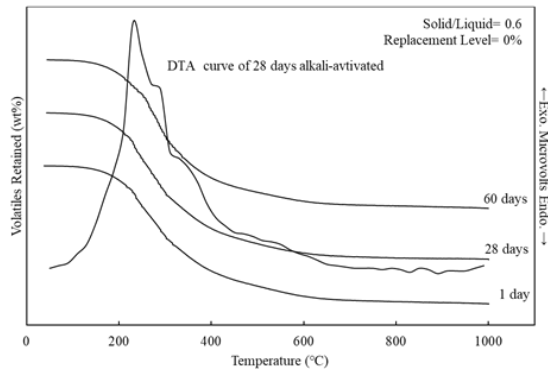
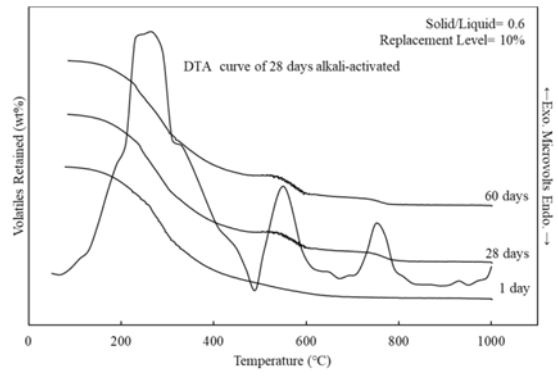


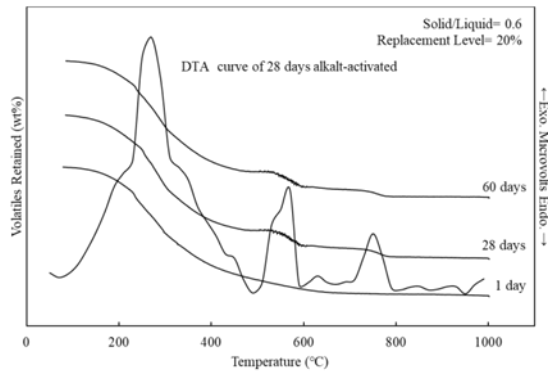
Fig. 3. TG/DTA curves of LCD waste glass geopolymers at S/L ratio of 0.4: (a) Replacement Level= 0%, (b) Replacement Level= 10%, (c) Replacement Level= 20%, (d) Replacement Level= 30% and (e) Replacement Level= 40%



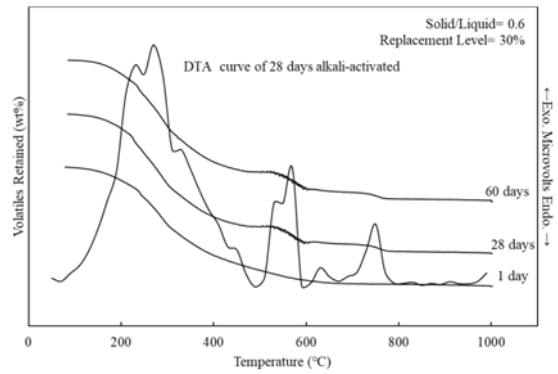
(a) Replacement Level= 0%



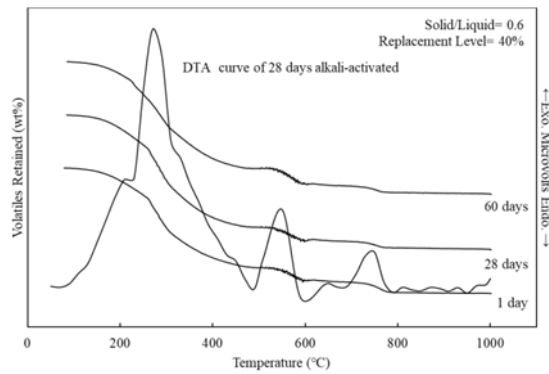
(b) Replacement Level= 10%



(c) Replacement Level= 20%

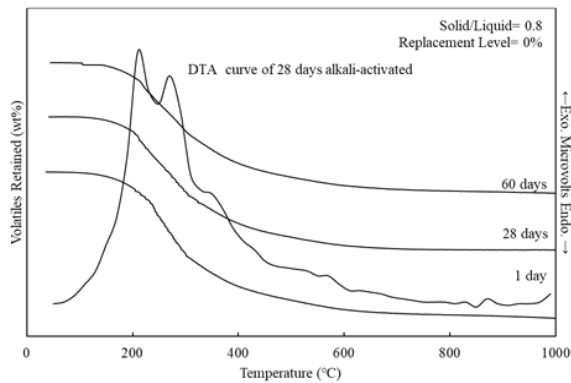


(d) Replacement Level= 30%

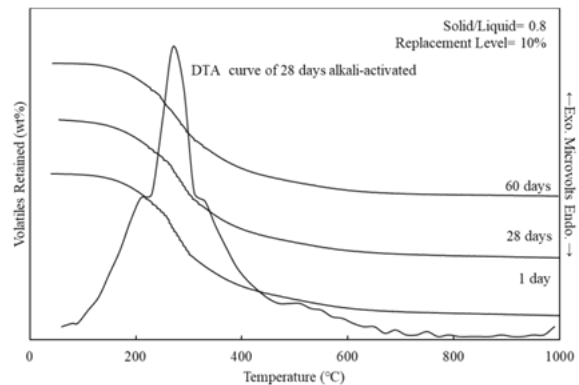


(e) Replacement Level= 40%

Fig. 4. TG/DTA curves of LCD waste glass geopolymers at S/L ratio of 0.6: (a) Replacement Level= 0%, (b) Replacement Level= 10%, (c) Replacement Level= 20%, (d) Replacement Level= 30% and (e) Replacement Level= 40%



(a) Replacement Level= 0%



(b) Replacement Level= 10%

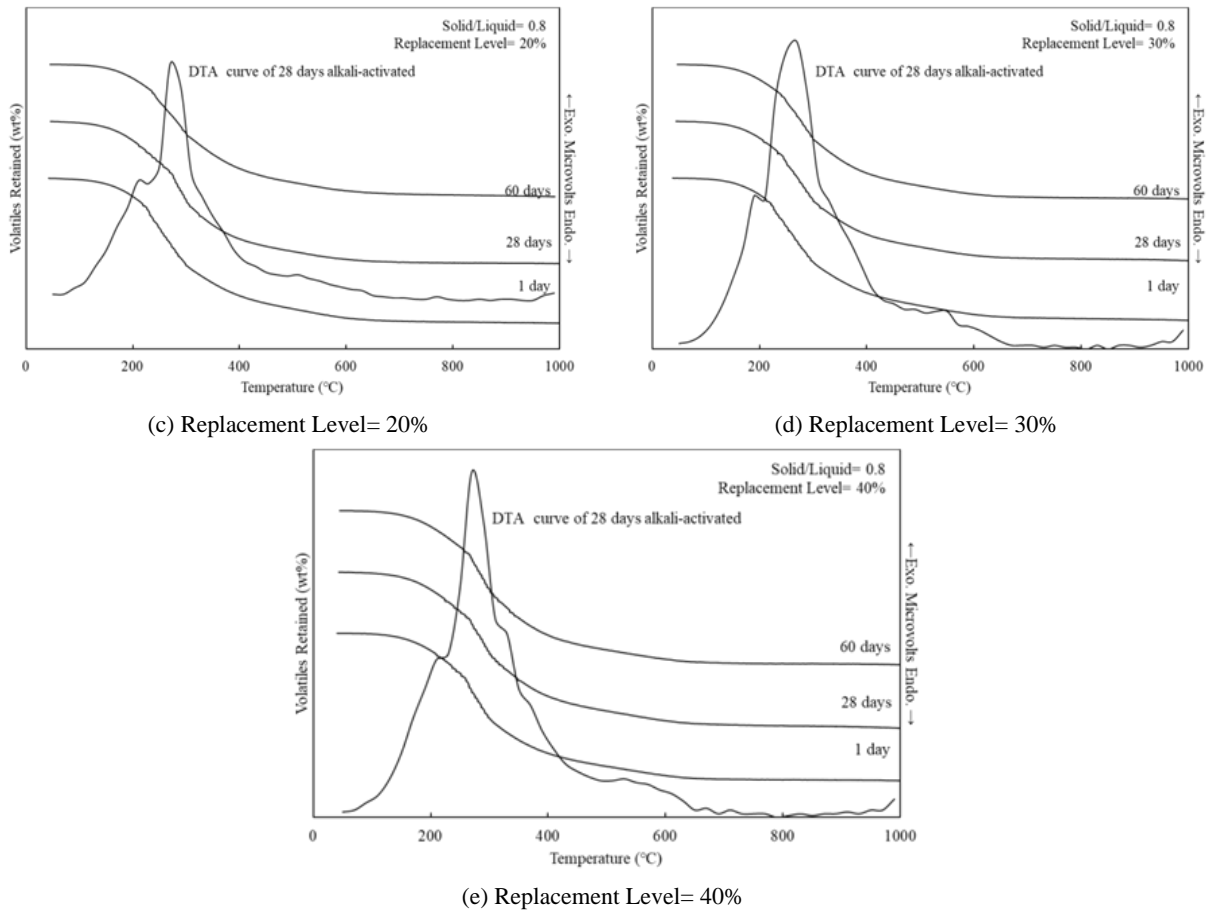
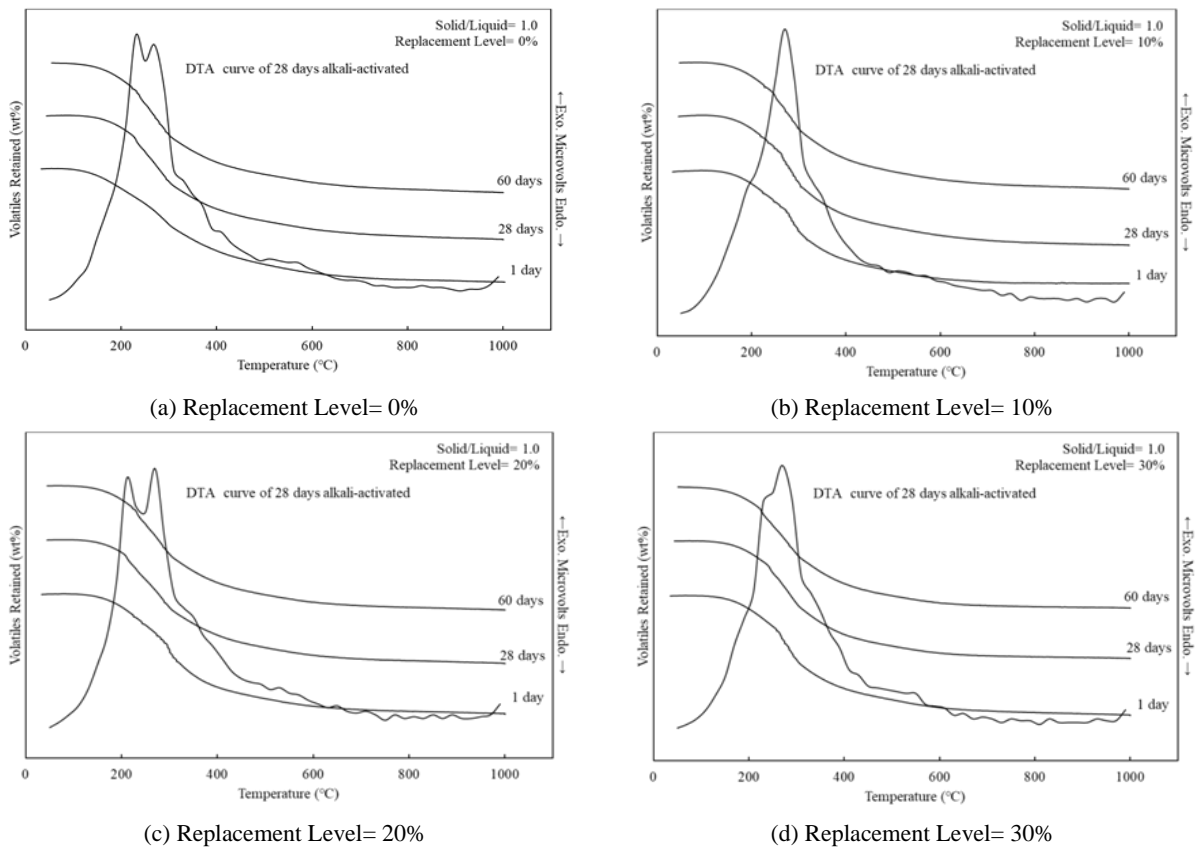
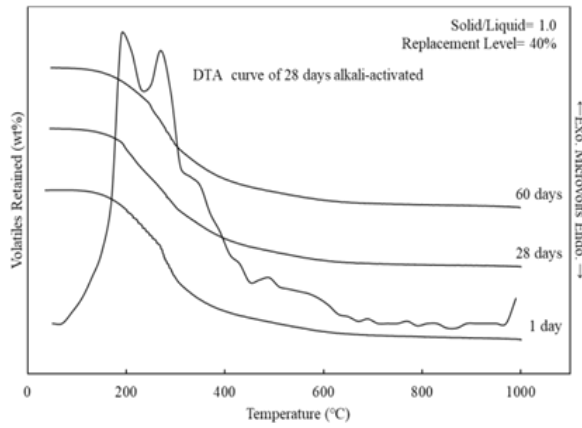


Fig. 5. TG/DTA curves of LCD waste glass geopolymers at S/L ratio of 0.8: (a) Replacement Level= 0%, (b) Replacement Level= 10%, (c) Replacement Level= 20%, (d) Replacement Level= 30% and (e) Replacement Level= 40%





(e) Replacement Level= 40%

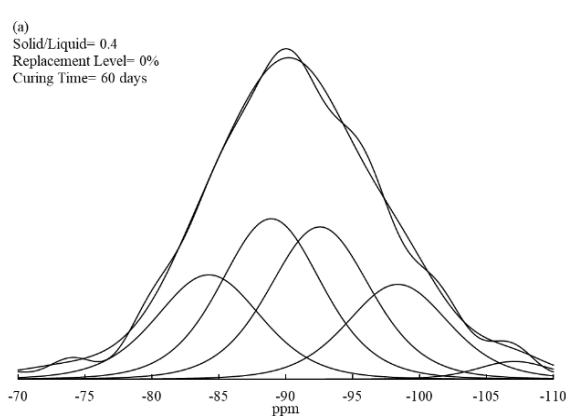
Fig. 6. TG/DTA curves of LCD waste glass geopolymers at S/L ratio of 1.0: (a) Replacement Level= 0%, (b) Replacement Level= 10%, (c) Replacement Level= 20%, (d) Replacement Level= 30% and (e) Replacement Level= 40%

The ^{27}Al NMR spectrum and deconvolution of LCD waste glass clay polymer at S/L of 0.4 are shown in Figure 7. The results showed that after 60 days of curing, the level of geopolymers in LCD waste glass replacement level increased from 0% to 40%, and the peak of $\text{Q}^4(3\text{Al})$ was -88.92 to -88.99 ppm. After 60 days of curing, as the LCD waste glass replacement level increased (Fig. 7), the peak in the NMR analysis shifted to the right side, indicating that few silicon tetrahedrons are coordinated to aluminum tetrahedrons (Rahier et al., 1996; Wan et al., 2017). As the S/L ratio was increased from 0.4 to 0.6, after a curing time of 60 days, the peak intensity of $\text{Q}^4(3\text{Al})$ of the geopolymers with 10% LCD waste glass replacement level increased by 157%, as shown in Fig. 8(b). Lo et al. indicated that the geopolymers showed high percentages of $\text{Q}^4(3\text{Al})$, indicating high initial levels of aluminosilicate (Lo et al., 2019). Furthermore, when the LCD waste glass content is 40% of the geopolymer, compared with the LCD waste glass content of 10%, the peak intensity drops sharply by 60.8% (Figure 8 (b) and Figure 8 (e)). This

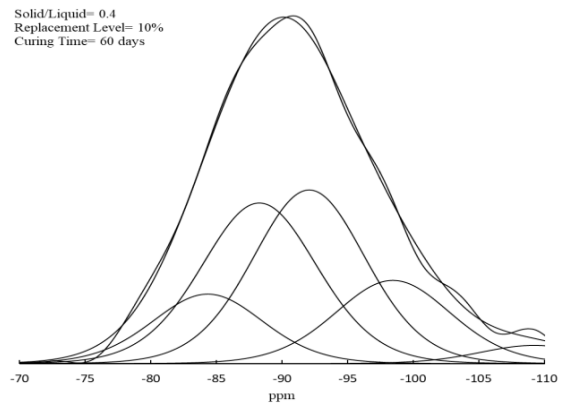
effect is due to the reduction in the release of silicon and aluminum ions from waste glass, causing the peak intensity decreased.

For the geopolymers with 10% LCD waste glass at 60-day of curing, the peak center of -88.32 ppm had shifted to -88.12 ppm when the S/L ratio increased from 0.6 to 1.0, indicating that more aluminum tetrahedrons were coordinated to the silicon tetrahedrons, as shown in Figs. 8–10. When the S/L ratio was increased, the silica content in the system was high. The increase in the silica content enhanced the geopolymer synthesis reaction. At an S/L ratio of 1.0, the concentrations of aluminate and silicate monomers were suitable for developing geopolymer gels in the microstructural forms of $\text{Q}^4(2\text{Al})$ and $\text{Q}^4(3\text{Al})$.

Therefore, when the S/L ratio increased from 0.6 to 1.0, for the geopolymers with 10% LCD waste glass, compared to geopolymers with an S/L ratio of 0.8, the peak intensities of $\text{Q}^4(3\text{Al})$ and $\text{Q}^4(2\text{Al})$ increased by 102% and 113%, respectively. (Fig. 9(b)).



(a) Replacement Level= 0%



(b) Replacement Level= 10%

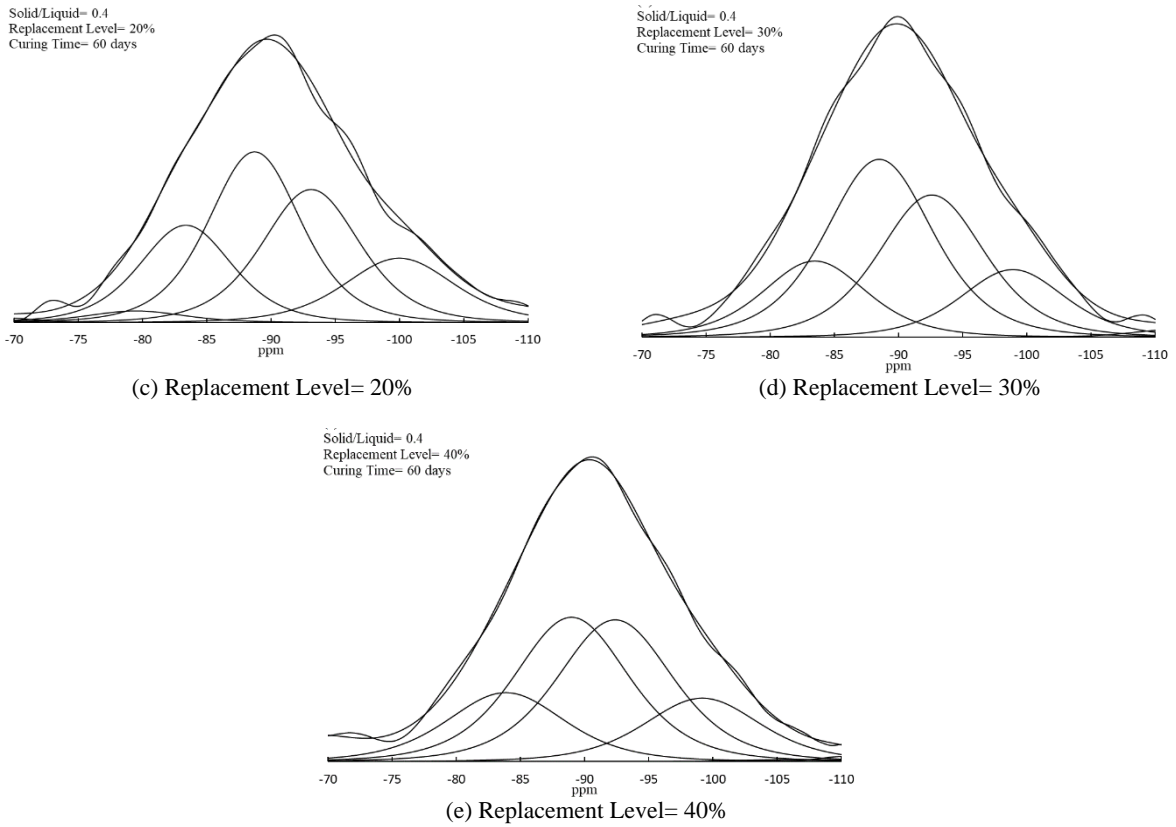
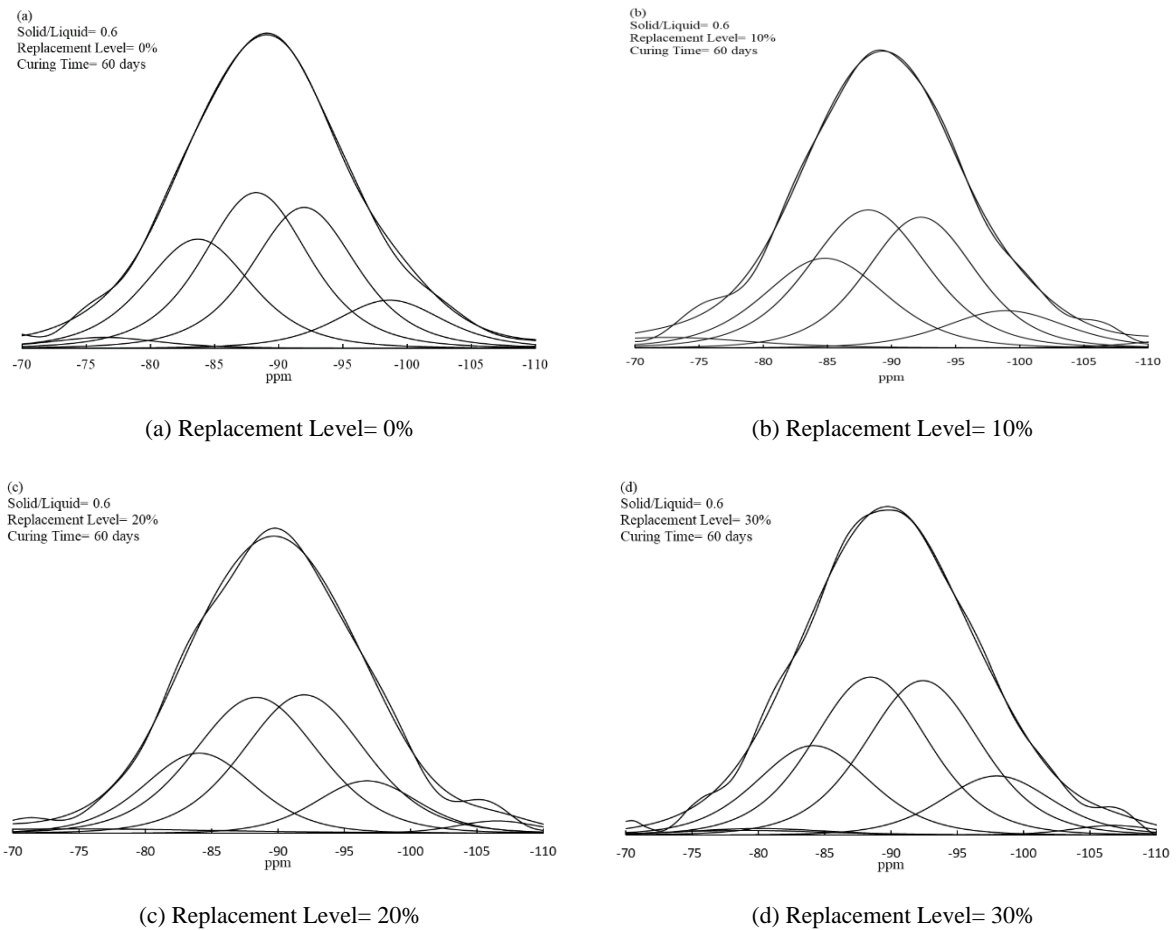
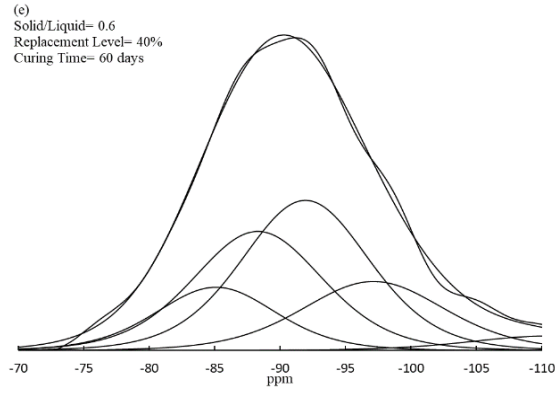


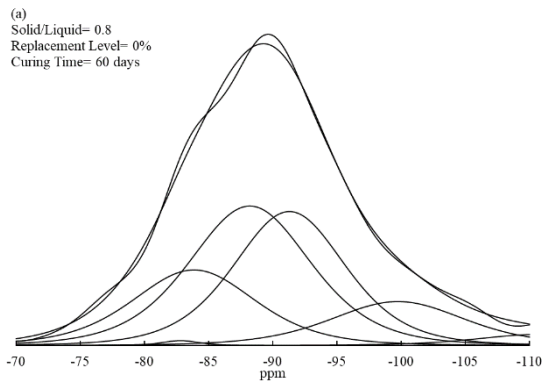
Fig. 7. The ^{27}Al NMR spectra and deconvolutions of LCD waste glass geopolymers at S/L ratio of 0.4: (a) Replacement Level= 0%, (b) Replacement Level= 10%, (c) Replacement Level= 20%, (d) Replacement Level= 30% and (e) Replacement Level= 40%



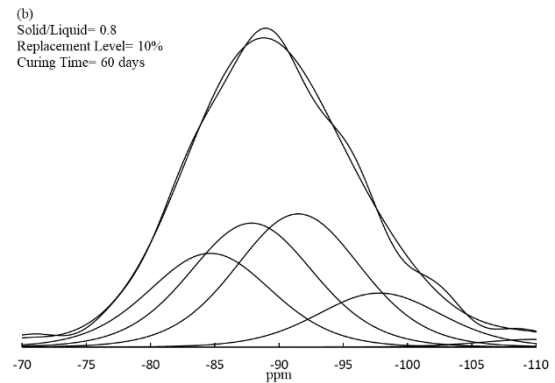


(e) Replacement Level= 40%

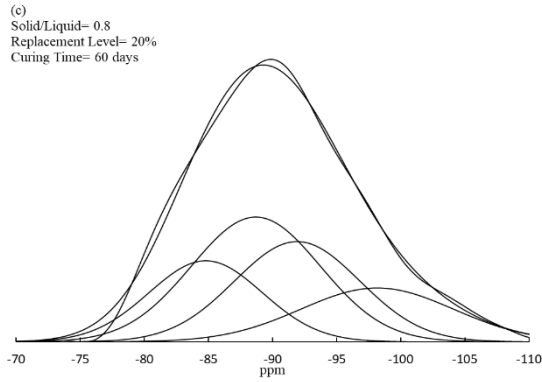
Fig. 8. The ^{27}Al NMR spectra and deconvolutions of LCD waste glass geopolymers at S/L ratio of 0.6: (a) Replacement Level= 0%, (b) Replacement Level= 10%, (c) Replacement Level= 20%, (d) Replacement Level= 30% and (e) Replacement Level= 40%



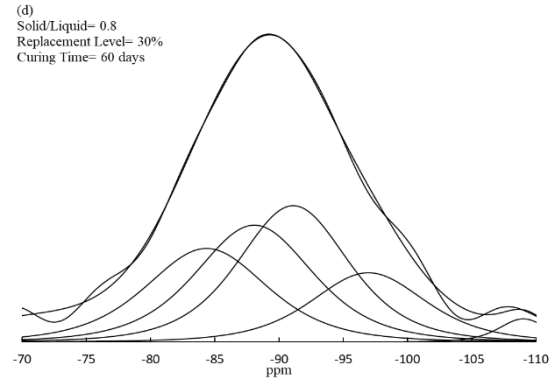
(a) Replacement Level= 0%



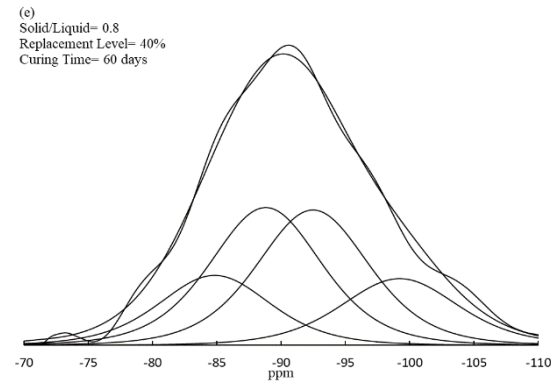
(b) Replacement Level= 10%



(c) Replacement Level= 20%



(d) Replacement Level= 30%



(e) Replacement Level= 40%

Fig. 9. The ^{27}Al NMR spectra and deconvolutions of LCD waste glass geopolymers at S/L ratio of 0.8: (a) Replacement Level= 0%, (b) Replacement Level= 10%, (c) Replacement Level= 20%, (d) Replacement Level= 30% and (e) Replacement Level= 40%

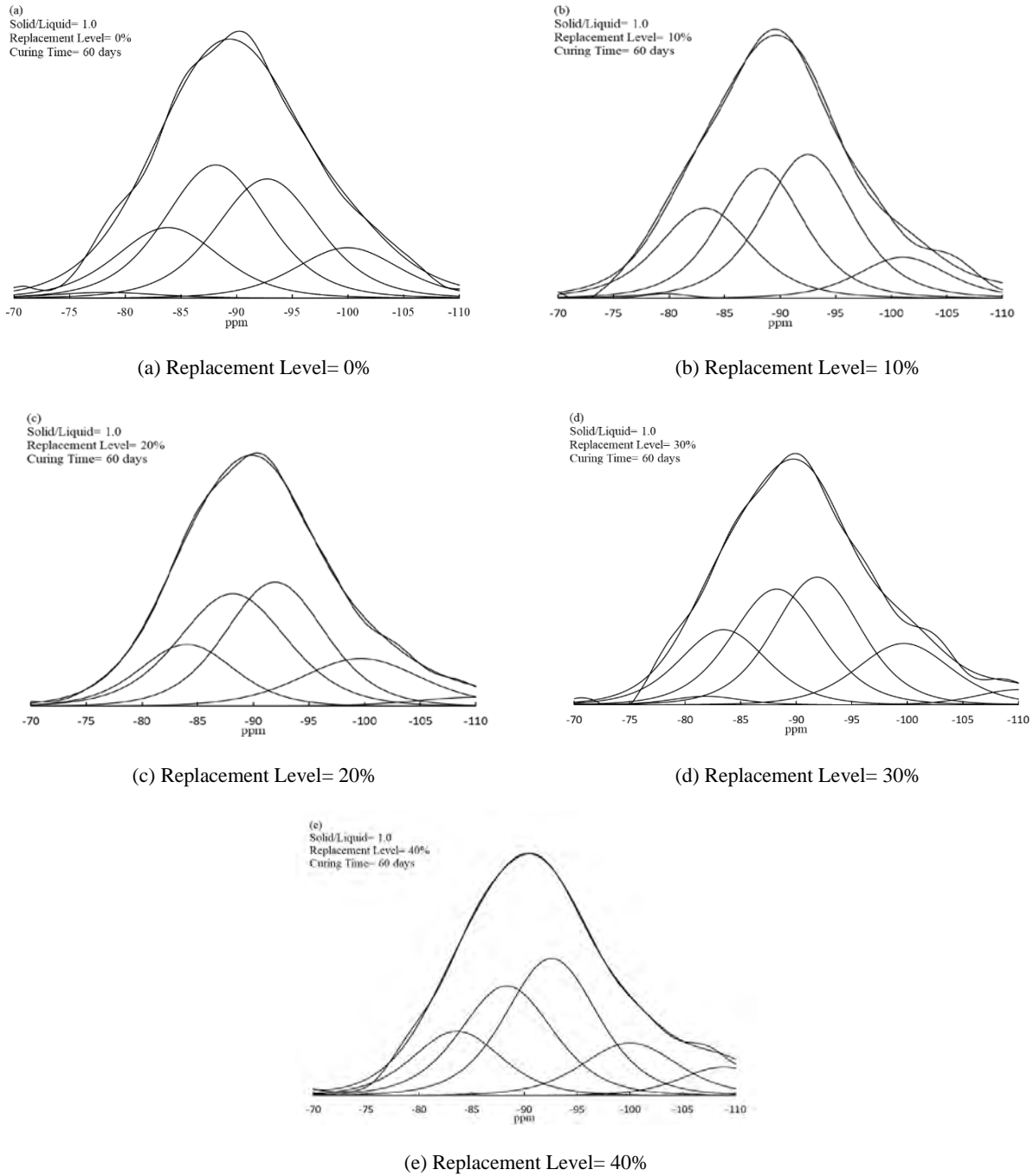


Fig. 10. The ²⁷Al NMR spectra and deconvolutions of LCD waste glass geopolymers at S/L ratio of 1.0: (a) Replacement Level= 0%, (b) Replacement Level= 10%, (c) Replacement Level= 20%, (d) Replacement Level= 30% and (e) Replacement Level= 40%

Fig. 11 presents the deconvoluted fractions of silicon centers geopolymers with an S/L ratio of 0.4, the main elements of Q⁴ (3Al) and Q⁴ (2Al) in LCD waste glass increased, and there were trace amounts of Q⁴ (4Al) compounds. With the replacement of LCD waste glass from 20% to 40%, the fractions of Q⁴(3Al) (34.44% to 34.01%) decrease, and the fractions of Q⁴(4Al) (16.72% to 19.65%) and Q⁴(1Al) (14.61% to 18.82%) increase. Wan (2017) indicated the geopolymers with deconvoluted integrals of Q⁴ (1Al), Q⁴ (2Al), and Q⁴ (3Al) may be geopolymer gels, while Q⁴ (0Al) and Q⁴ (4Al) have low scores. might be silicate derivatives and zeolite nuclei, respectively (Wan et al., 2017).

The results show that when the replacement level of LCD waste glass is high, the content of LCD waste glass will increase caused unsatisfactory oligomers to form geopolymer gel decreased, thus causing the fractions amounts of Q⁴(3Al) decreased. For the reason that the fractions of Q⁴(4Al) and Q⁴(1Al) increase, as shown in Fig. 11(a) and Fig. 11(d). Fig. 12 shows the fraction of Q⁴ (0Al–4Al) silicon ion center (%) of the LCD waste glass geopolymer has an S / L ratio of 0.6. After curing for 1 day, in the geopolymer with a replacement rate of 10% of the LCD waste glass, the percentages of Q⁴ (3Al), Q⁴ (2Al) and Q⁴ (1Al) were 34.22%, 31.10% and 11.20%, respectively.

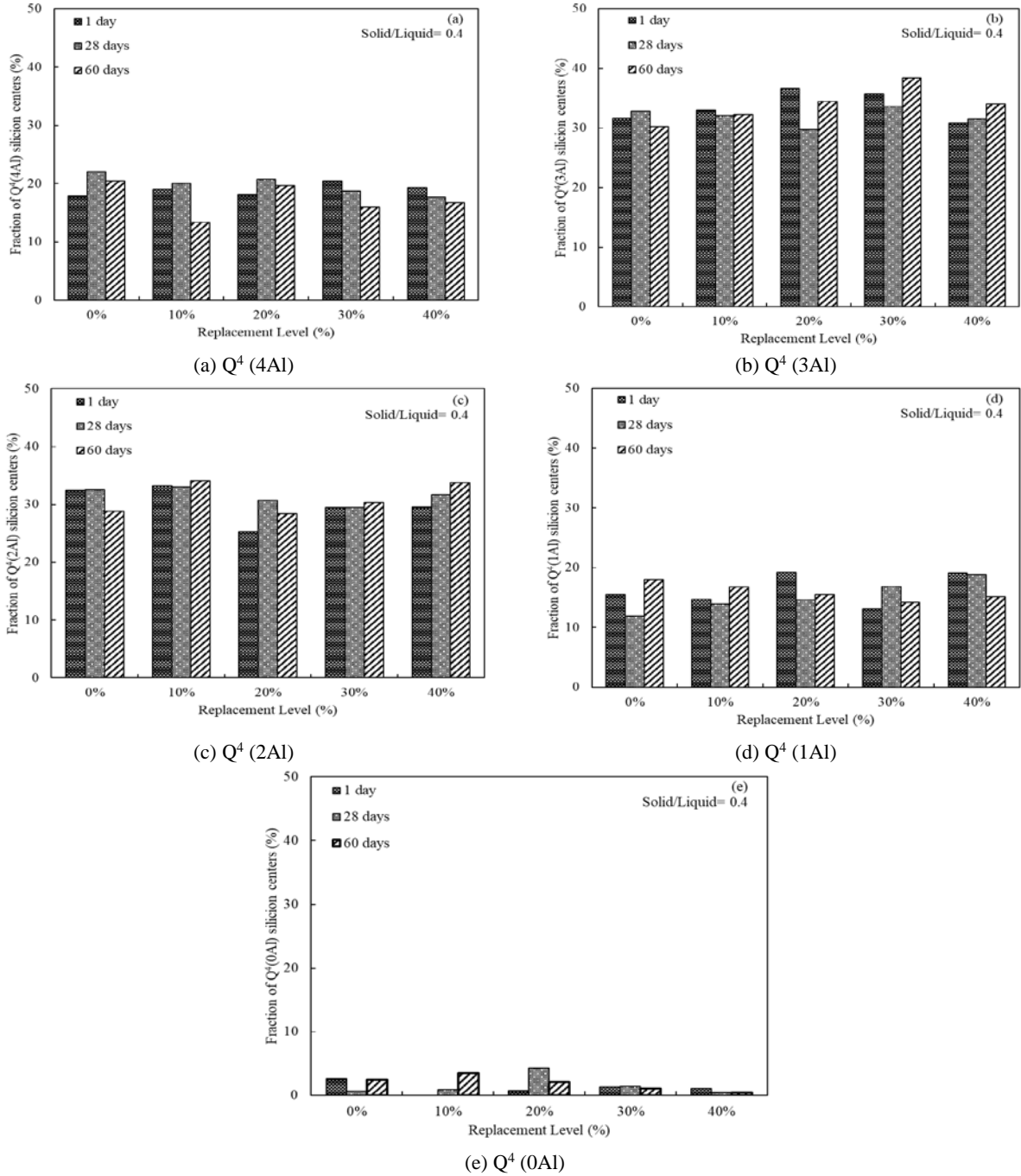


Fig. 11. The Fraction of Q⁴ (0Al–4Al) silicium centers (%) of LCD waste glass geopolymers at S/L ratio of 0.4: (a) Q⁴ (4Al), (b) Q⁴ (3Al), (c) Q⁴ (2Al), (d) Q⁴ (1Al) and (e) Q⁴ (0Al)

After curing for 60 days, the percentages of Q⁴ (3Al), Q⁴ (2Al) and Q⁴ (1Al) were 35.07%, 30.40% and 9.57%, respectively. The results show that the proportion of silicide centers in the fourth quarter (%) contents of geopolymer increased with the increase the curing time. This performance could be attributed, the reactivity of the geopolymers by forming amorphously geopolymeric structured, which is similar to the Wan et al., report (Wan et al., 2017). Fig. 13 and Fig. 14 present the fraction of Q⁴(0Al–4Al) silicium centers (%) of LCD waste glass geopolymers with S/L ratios of 0.8 and 1.0, respectively.

It is indicate that when increase in S/L ratio from 0.8 to 1.0 in geopolymers with 10% LCD waste glass cured for 60 days increases fractions of Q⁴(3Al) (30.06%–30.13%) and Q⁴(2Al) (32.52%–35.13%), and Q⁴(1Al) (13.14%–10.15%) (Figs. 13(b)-(d) and Figs. 14(b)-(d)). Due to the increase in oligomer size due to the S/L ratio, which the concentrations of aluminate and silicate monomers were suitable for developing geopolymer gels of the deconvoluted fractions of Q⁴(1Al), Q⁴(2Al) and Q⁴(3Al) (Wan et al., 2017). When the S/L ratios of 1.0, in geopolymer with LCD waste glass replacement level of 20% at the 60

day of curing, the percentages of Q^4 (3Al), Q^4 (2Al), and Q^4 (1Al) were 32.69%, 33.08%, and 15.48%, respectively (Figure 14 (b)-(d)). The results show that as the content of LCD waste glass increases by 20%, the Q^4 (3Al), Q^4 (2Al) and Q^4 (1Al) percentages of geopolymers increase. Because the chemically reactive CaO content in the LCD waste glass, heterogeneous nucleation-crystallization may occur, which promoted the geopolymerization to form amorphously geopolymeric products. Therefore, the fraction of Q^4 silicium centers (%) contents of geopolymers with 20% LCD waste glass increased. These results are favorable for flexural strength development.

3.4. Discussion

As shown in Fig. 2, the flexural strength of geopolymer samples at the S/L ratio =0.4 are in all

cases lower those at different S/L ratios. Cho et al. reported that fly ash-based geopolymer is evaluated considering four test variables covering Na_2O content, SiO_2/Na_2O molar ratios, curing temperature/period, and pre-curing temperature/period (Cho et al., 2017). With increasing Na_2O content in the activator solution, the solubility of silica and alumina in fly ash increased, but the amount of silica and alumina dissolved in fly ash increased. are limited, it is due to precipitations of geopolymer gels around the surface of fly ash particles (Cho et al., 2017).

From the results, it is known that when S/L ratio is relatively low, when OH^- increased, the solubility is increased led to accelerate the condensation as shown from the TG/DTA and ^{27}Al NMR spectra results (Table 1 and Fig. 6), but the polycondensation is inhibited, it is led to reduces mechanical strength (Fig. 2), which is similar to the Cho et al. report (Cho et al., 2017).

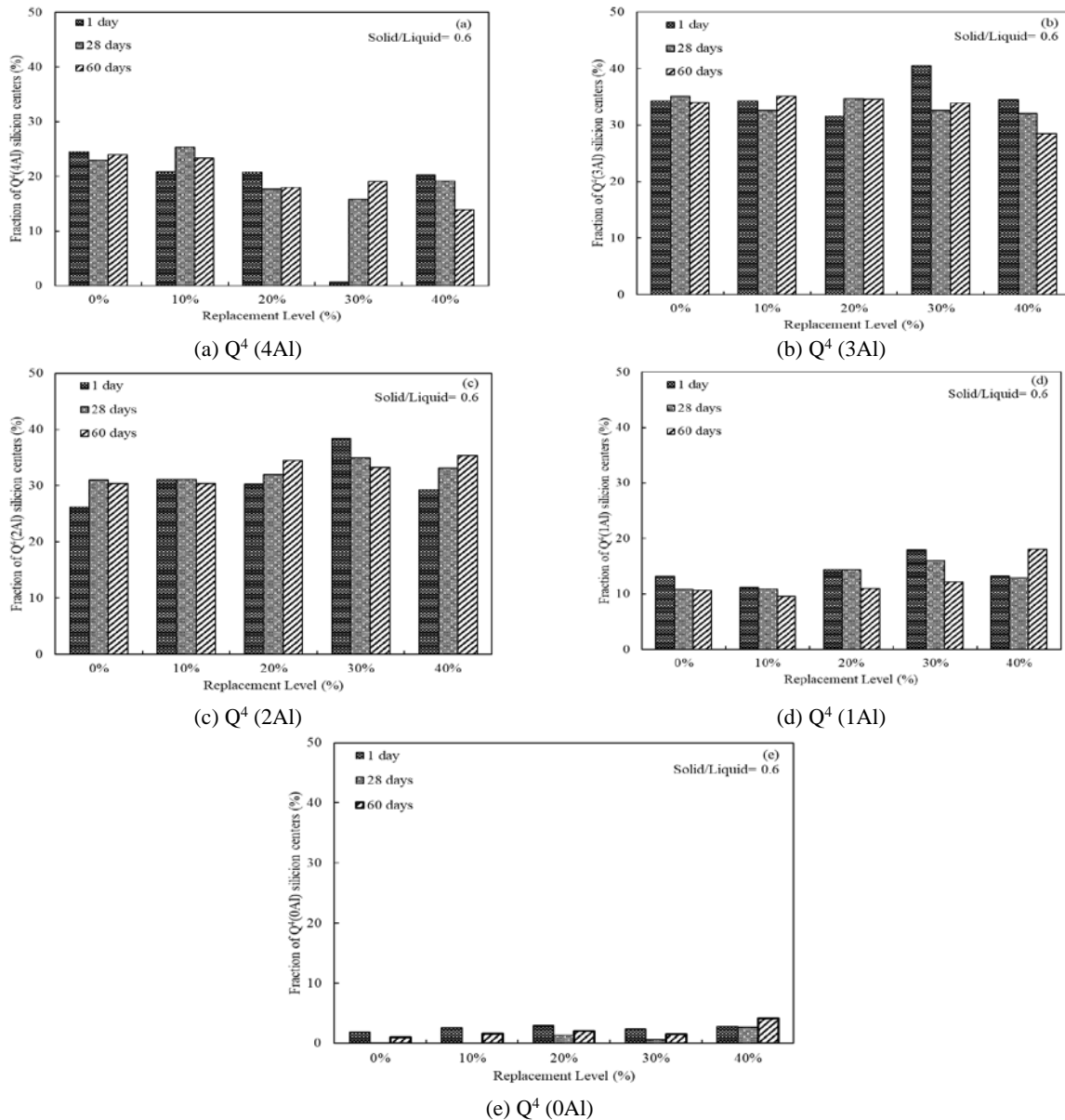


Fig. 12. The Fraction of Q^4 (0Al-4Al) silicium centers (%) of LCD waste glass geopolymers at S/L ratio of 0.6: (a) Q^4 (4Al), (b) Q^4 (3Al), (c) Q^4 (2Al), (d) Q^4 (1Al) and (e) Q^4 (0Al)

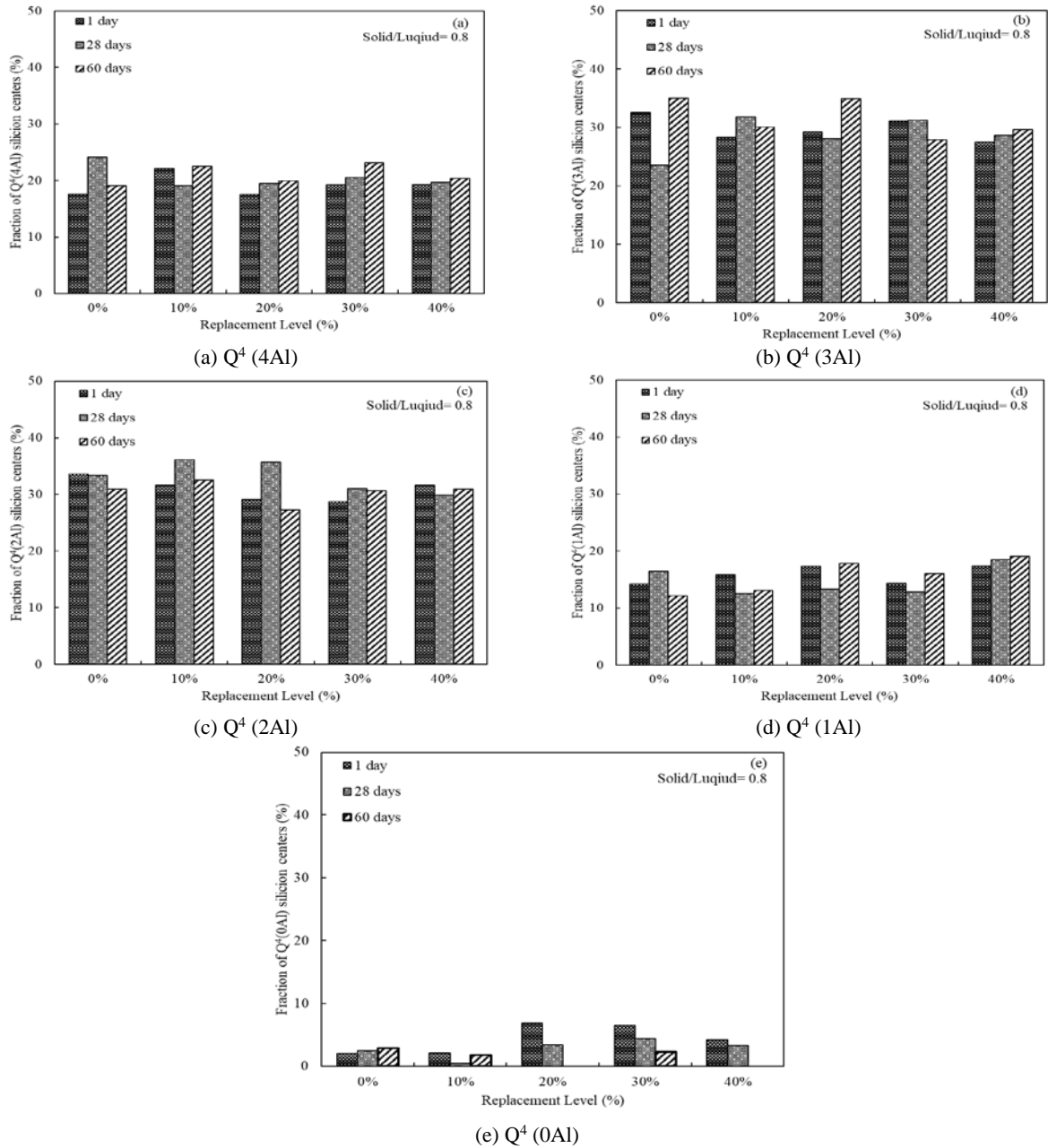
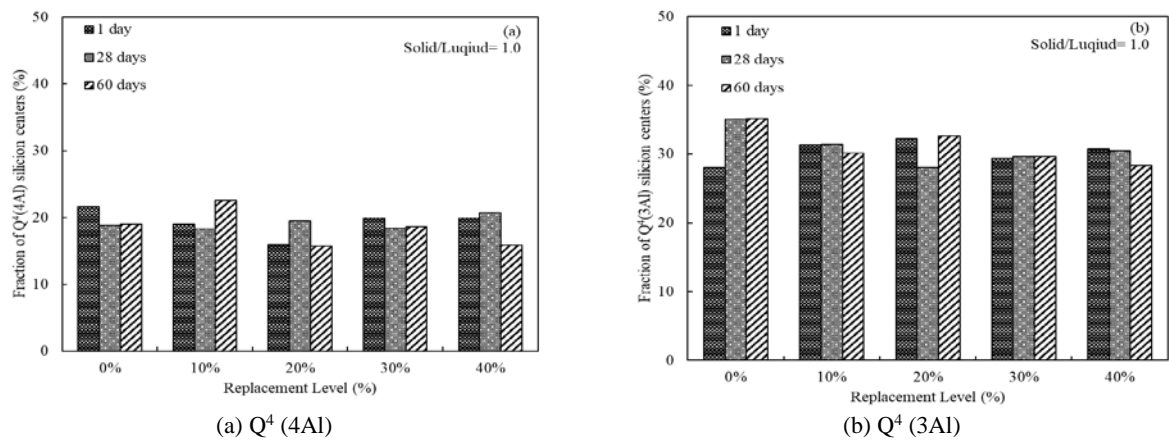


Fig. 13. The Fraction of Q^4 (0Al–4Al) silicium centers (%) of LCD waste glass geopolymers at S/L ratio of 0.8: (a) Q^4 (4Al), (b) Q^4 (3Al), (c) Q^4 (2Al), (d) Q^4 (1Al) and (e) Q^4 (0Al)



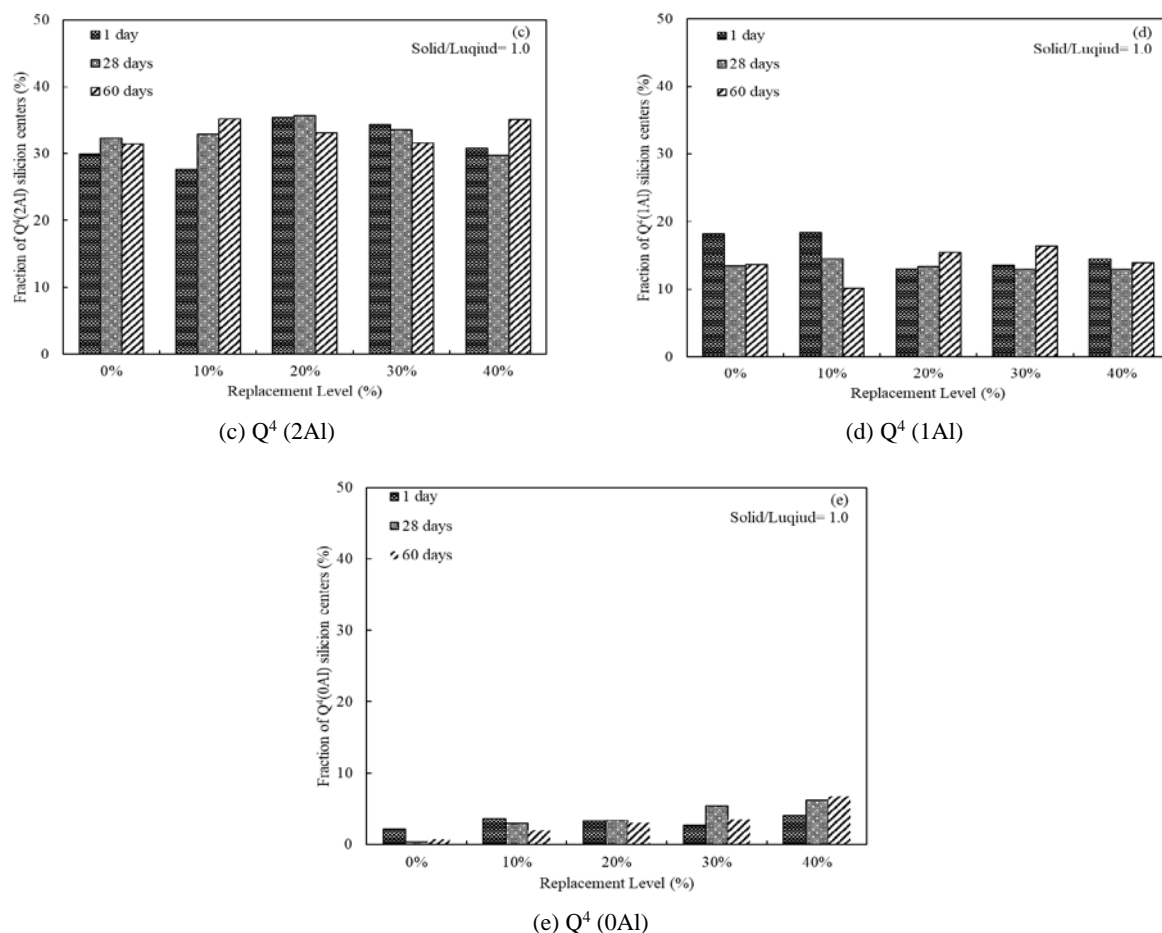


Fig. 14. The Fraction of Q⁴ (0Al–4Al) silicium centers (%) of LCD waste glass geopolymers at S/L ratio of 1.0: (a) Q⁴ (4Al), (b) Q⁴ (3Al), (c) Q⁴ (2Al), (d) Q⁴ (1Al) and (e) Q⁴ (0Al)

On the other hand, the silica content in the system was high that may lead to densification of geopolymer which favors mechanical strength (Lo et al., 2019). As a result, the flexural strength of the geopolymer samples increased with increasing S/L ratio (Fig. 2). Increasing the S/L ratio results in an increase in the size of oligomers, affecting the kinetics of the exchange of silicate units between species during geopolymerization, it is led to the silica content in the system increased and in turn enhanced the geopolymer synthesis reaction. LCD waste glass geopolymer with deconvoluted fractions of Q⁴(1Al+2Al+3Al) might be geopolymer gels, and low fractions of Q⁴(0Al) and Q⁴(4Al) might be silicate derivatives and zeolite nuclei. On the other hand, the silica content in the system was high that may lead to densification of geopolymer which favourable mechanical strength.

4. Conclusions

The flexural strength of the geopolymer samples increased with increasing S/L ratio. Increasing the S/L ratio results in an increase in the size of oligomers, it is led to the silica content in the system increased and in turn enhanced the geopolymer synthesis reaction. In the temperature range of 230–400°C, when the LCD content in the geopolymer is

10%, the S / L ratio after curing for 60 days is 0.6. Due to the enhancement of polymerization, the weight loss is relative to the S / L ratio of 0.4. Increased S / L ratio for higher responses.

At an S/L ratio of 1.0, the concentrations of aluminate and silicate monomers were suitable for the development of Q⁴ (2Al+3Al) microstructured geopolymer gels. According to the results of the flexural strength, the substitution rate of metakaolin polymer and LCD waste glass with S / L of 1.0 is 10%, resulting in more favorable mechanical properties and microstructure (TG/DTA, and NMR analyses). Geopolymer with 10%–40% LCD waste glass and a solid/liquid ratio of 1.0 can partially replace metakaolin as geopolymer exhibit favourable mechanical characteristics.

References

- Allahverdi A., Vafaei M., Maghsoodloorad H., (2017), Quality control and assessment of geopolymer cements based on reacted and free alkalis, *Construction and Building Materials*, **153**, 274–283.
- Bai C., Zheng J., Rizzi G.A., Colombo P., (2018), Low-temperature fabrication of SiC/geopolymer cellular composites, *Composites Part B*, **137**, 23–30.
- Bai C.Y., Li H.Q., Bernardo E., Colombo P., (2019), Waste-to-resource preparation of glass-containing foams from geopolymers, *Ceramics International*, **45**, 7196–7202.

- Bergamonti L., Taurino R., Cattani L., Ferretti D., Bondioli F., (2018), Lightweight hybrid organic-inorganic geopolymers obtained using polyurethane waste, *Construction and Building Materials*, **185**, 285-292.
- Chen Y., Li S.T., Tan Q.Y., Li J.H., Miao Y.P., (2019), Study on WEEE collection and recycling scheme in typical Asia-Pacific countries, *Environmental Engineering and Management Journal*, **18**, 1487-1498.
- Cheng Y.M., Hongyu C., Jiaxin W., Jing S., Zonghui L., Mingkai Y., (2018), Preparation and characterization of coal gangue geopolymers, *Construction and Building Materials*, **187**, 318-326.
- Cho Y.K., Yoo S.W., Jung S.H., Lee K.M., Kwon S.J., (2017), Effect of Na₂O content, SiO₂/Na₂O molar ratio, and curing conditions on the compressive strength of FA-based geopolymer, *Construction and Building Materials*, **145**, 253-260.
- Dembovska L., Bajare D., Ducman V., Korat L., Bumanis G., (2017), The use of different by-products in the production of lightweight alkali activated building materials, *Construction and Building Materials*, **135**, 315-322.
- Duxson P., Fernández-Jiménez A., Provis J.L., Lukey G.C., Palomo A., van Deventer J.S.J., (2007), Geopolymer technology: the current state of the art, *Journal of Materials Science*, **42**, 2917-2933.
- El-Naggar M.R., El-Dessouky M.I., (2017), Re-use of waste glass in improving properties of metakaolin-based geopolymers: Mechanical and microstructure examinations, *Construction and Building Materials*, **132**, 543-555.
- Elyamany H.E., Elmoaty A.E.M.A., Elshaboury A.M., (2018), Magnesium sulfate resistance of geopolymer mortar, *Construction and Building Materials*, **184**, 111-127.
- Fan C.S., Li K.C., (2013), Production of insulating glass ceramics from thin film transistor-liquid crystal display (TFT-LCD) waste glass and calcium fluoride sludge, *Construction and Building Materials*, **57**, 335-341.
- Fernández-Pereir C., Luna-Galiano Y., Pérez-Clemente M., Leiv C., Arroyo F., Villegas R., Vilches L.F., (2018), Immobilization of heavy metals (Cd, Ni or Pb) using aluminate geopolymers, *Materials Letters*, **227**, 184-186.
- Gao K., Lin K.L., Hwang C.L., Tuan B.L.A., Cheng T.W., Wang D., (2018), Elucidating the effects of nanosilica on the characteristics of alkali-activated thin-film transistor liquid-crystal display waste glass, *Environmental Engineering and Management Journal*, **17**, 293-306.
- Ghadir P., Ranjbar N., (2018), Clayey soil stabilization using geopolymer and Portland cement, *Construction and Building Materials*, **188**, 361-371.
- Hao H.C., Lin K.L., Wang D.Y., Chao S.J., Shiu H.S., Cheng T.W., Hwang C.L., (2015), Elucidating characteristics of geopolymer with solar panel waste glass, *Environmental Engineering and Management Journal*, **14**, 79-87.
- Leay L., Potts A., Donoclift T., (2018), Geopolymers from fly ash and their gamma irradiation, *Materials Letters*, **227**, 240-242.
- Lee S.K., Stebbins J.F., (1999), The degree of aluminum avoidance in aluminosilicate glasses, *American Mineralogist*, **84**, 937-945.
- Lin K.L., Shiu H.S., Shie J.L., Cheng T.W., Hwang C.L., (2012), Effect of composition on characteristics of thin film transistor liquid crystal display (TFT-LCD) waste glass-metakaolin-based geopolymers, *Construction and Building Materials*, **36**, 501-507.
- Lo K.W., Lin K.L., Cheng T.W., Shiu H.S., (2018), Effect of alkali activation thin film transistor-liquid crystal display waste glass on the mechanical behavior of geopolymers, *Construction and Building Materials*, **162**, 724-731.
- Lo K.W., Lin K.L., Cheng T.W., Zhang B.X., (2019), The influence of sapphire substrate silicon carbide sludge on structural properties of metakaolin-based geopolymers, *Environmental Progress & Sustainable Energy*, 1-12.
- Ma C.K., Awang A.Z., Omar W., (2018), Structural and material performance of geopolymer concrete: A review, *Construction and Building Materials*, **186**, 90-102.
- Novais R.M., Ascensão G., Seabra M.P., Labrincha J.A., (2016), Waste glass from end-of-life fluorescent lamps as raw material in geopolymers, *Waste Management*, **52**, 245-255.
- Rahier H., Van Mele B., Biesemans M., Wastiels J., Wu X., (1996), Low-temperature synthesized aluminosilicate glasses, *Journal of Materials Science*, **31**, 71-79.
- Tadashi U., (2016), LCD Glass Area Demand to Rise 13 Percent from 2015 to 2018, IHS Says, IHS Markit Press Release, 23. 05. 2016, Englewood, Colorado, On line at: <https://technology.ihs.com/575798/lcd-glass-area-demand-to-rise-13-percent-from-2015-to-2018-ihs-says>.
- Tang N., Deng Z., Daic J.G., Yang K., Chen C., Wang Q., (2018), Geopolymer as an additive of warm mix asphalt: Preparation and properties, *Journal of Cleaner Production*, **192**, 906-915.
- Villaquirán-Cacedo M.A., Mejía de Gutiérrez R., (2018), Synthesis of ceramic materials from ecofriendly geopolymer precursors, *Materials Letters*, **230**, 300-304.
- Wan Q., Rao F., Song S.X., (2017a), Reexamining calcination of kaolinite for the synthesis of metakaolin geopolymers-roles of dehydroxylation and recrystallization, *Journal of Non-Crystalline Solid*, **460**, 74-80.
- Wan Q., Rao F., Song S.X., García R.E., Estrella R.M., Patiño C.L., Zhang Y., (2017b), Geopolymerization reaction, microstructure and simulation of metakaolin-based geopolymers at extended Si/Al ratios, *Cement and Concrete Composites*, **79**, 45-52.
- Wang W.C., Wang H.Y., Tsai H.C., (2016), Study on engineering properties of alkali-activated ladle furnace slag geopolymer, *Construction and Building Materials*, **123**, 800-805.